ORIGINAL RESEARCH

Neuronal $Na_v1.8$ Channels as a Novel Therapeutic Target of Acute Atrial Fibrillation Prevention

XiaoMeng Chen, MD;* LiLei Yu, MD, PhD;* ShaoBo Shi, MD, PhD; Hong Jiang, MD, PhD; CongXin Huang, MD, PhD; Mayurika Desai, MS; YiGang Li, MD, PhD; Hector Barajas-Martinez, PhD; Dan Hu, MD, PhD

***Background*—**Ganglionated plexus have been developed as additional ablation targets to improve the outcome of atrial fibrillation (AF) besides pulmonary vein isolation. Recent studies implicated an intimate relationship between neuronal sodium channel $Na_v1.8$ (encoded by *SCN10A*) and AF. The underlying mechanism between $Na_v1.8$ and AF remains unclear. This study aimed to determine the role of $Na_v1.8$ in cardiac electrophysiology in an acute AF model and explore possible therapeutic targets.

***Methods and Results*—**Immunohistochemical study was used on canine cardiac ganglionated plexus. Both $Na_v1.5$ and $Na_v1.8$ were expressed in ganglionated plexus with canonical neuronal markers. Sixteen canines were randomly administered either saline or the $Na_v1.8$ blocker A-803467. Electrophysiological study was compared between the 2 groups before and after 6-hour rapid atrial pacing. Compared with the control group, administration of A-803467 decreased the incidence of AF (87.5% versus 25.0%, $P<0.05$), shortened AF duration, and prolonged AF cycle length. A-803467 also significantly suppressed the decrease in the effective refractory period and the increase in effective refractory period dispersion and cumulative window of vulnerability caused by rapid atrial pacing in all recording sites. Patch clamp study was performed under 100 nmol/L A-803467 in TSA201 cells cotransfected with *SCN10A*-WT, *SCN5A*-WT, and *SCN3B*-WT. $I_{Na,P}$ was reduced by 45.34% at −35 mV, and $I_{Na,L}$ by 68.57% at −20 mV. Evident fast inactivation, slow recovery, and use-dependent block were also discovered after applying the drug.

***Conclusions*—**Our study demonstrates that $Na_v1.8$ could exert its effect on electrophysiological characteristics through cardiac ganglionated plexus. It indicates that $Na_v1.8$ is a novel target in understanding cardiac electrophysiology and *SCN10A*-related arrhythmias. **(*J Am Heart Assoc*. 2016;5:e004050 doi: 10.1161/JAHA.116.004050)**

Key Words: atrial fibrillation • electrophysiology • ganglionated plexus • $Na_v1.8$ • *SCN10A*

It has been recognized that cardiac autonomic nervous system activity is of great significance in the initiation and maintenance of atrial fibrillation (AF). Stimulation or inhibition of selective extracardiac neural structures may be a useful therapeutic option for cardiac arrhythmias, including AF, and other abnormalities. As the major part of the intrinsic cardiac autonomic nervous system, most cardiac ganglionated plexus (GPs) embedded in the fat pad around 4 pulmonary veins (PVs), play an important role in the early stage of AF.[1] Increased GP activity can induce the increase of both parasympathetic and sympathetic activity, which promotes rapid focal firing in the PV myocardium.[2,3] Clinical evidence also suggests that additional GP ablation to PV isolation could increase success rates in eliminating AF.[4,5]

As a tetrodotoxin-resistant periphery nerve voltage-gated sodium channel, $Na_v1.8$ (encoded by *SCN10A*) plays a significant part in the upstroke of action potential in neurons, and is responsible for repetitive firing.[6] It is found primarily expressed in small- and medium-diameter nociceptive sensory neurons, which mediate pain perception.[7] Genome-wide association study highlights the role of $Na_v1.8$ in cardiac conduction and arrhythmic diseases. In addition to the canonical cardiac sodium channel $Na_v1.5$/*SCN5A*, $Na_v1.8$ is recently considered a "new cardiac sodium channel."[8] *SCN10A* is adjacent to *SCN5A* on the same chromosome, and there is 70.4% of similarity in the amino acid sequence between these 2 sodium channels. Our previous research shows $Na_v1.8$ could physically interact with $Na_v1.5$ by using co-immunoprecipitation when both are expressed in vitro.[9]

From the Department of Cardiology, Xinhua Hospital, School of Medicine, Shanghai Jiao Tong University, Shanghai, China (X.C., Y.L.); Department of Cardiology and Cardiovascular Research Institute, Renmin Hospital of Wuhan University, Wuhan, China (L.Y., S.S., H.J., C.H., D.H.); Masonic Medical Research Laboratory, Utica, NY (M.D., H.B.-M., D.H.).

*Dr Chen and Dr Yu contributed equally to this work.

Correspondence to: Dan Hu, MD, PhD, Masonic Medical Research Laboratory, 2150 Bleecker Street, Utica, NY 13501-1787. E-mails: dianah@mmrl.edu; hudan0716@hotmail.com

Received June 8, 2016; accepted September 27, 2016.

Others prove that $Na_v1.8$ could modulate the activity and expression of $Na_v1.5$ at the transcriptional level, which may be intermediated by TBX3/5.[10,11]

Increasing evidence indicates that $Na_v1.8$/*SCN10A* plays a critical role in AF. Both common and rare variants of *SCN10A* were associated with the risk of AF.[12,13] Some rare *SCN10A* variants have been identified in patients with early-onset AF (rs141207048, rs202143516, rs202192818, rs139861061, et al), and the relevant mechanism implied by functional study in vitro might be through the modulation of peak sodium current ($I_{Na,P}$) and late sodium current ($I_{Na,L}$) of $Na_v1.8$.[14] Certain common variants, such as rs6795970, have been proved to be related to AF susceptibility.[12,13] One recent study has suggested that blockade of $Na_v1.8$ suppresses vagal-mediated AF most likely by inhibiting the neural activity of GP.[15] However, the exact electrophysiological role of $Na_v1.8$ in AF, especially at the early stage of acute AF, is uncertain, and the relevant mechanisms still need to be assessed. In this study, we aim to explore the expression of $Na_v1.8$ and $Na_v1.5$ in canine cardiac ganglia, and to evaluate the role of the $Na_v1.8$ blocker A-803467 in cardiac GP in an acute AF canine model. We have further investigated the changes of the channel density and kinetic characteristics in the presence of A-803467 when the *SCN5A* and *SCN10A* coexpressed in vitro, which might provide the potential mechanism to explain its effect in a canine AF model.

Methods

Animal Preparation

Experiments were approved by the Animal Ethics Committee of Wuhan University under approval number 2015-0072 and followed the guidelines outlined by the Care and Use of Laboratory Animals of the National Institutes of Health. Sixteen mongrel dogs weighing from 20 to 25 kg were included in this study. Surgeries were performed under anesthesia with sodium pentobarbital with an initial dose of 50 mg/kg and an additional dose of 2 mg/kg per hour. A heating pad was used to maintain the core body temperature at 36.5±1.5°C. All dogs were ventilated with room air by a positive pressure respirator. Bilateral thoracotomy was conducted at the fourth intercostal space, as previously described[16,17] (Figure 1A and 1B). In brief, multielectrode catheters were sutured to obtain recordings at the surface of the atrium and PVs and to pace at the left atrial appendage (LAA). All recordings were displayed on a computerized Bard Electrophysiology System (CR Bard Inc, Billerica, MA). High-frequency stimulation (20 Hz, 0.1 ms duration, square waves) was applied at the fat pad to identify GPs by a bipolar electrode stimulator (Grass-S88; Astro-Med, West Warwick, RI). Anterior right ganglionated plexi (ARGP) was located at the RSPV-atrial junction and superior left ganglionated plexi (SLGP) at the left superior PV (LSPV)-atrial junction. A successful GP stimulation was marked at the 50% sinus rate slowing or second- or third-degree atrioventricular block developing.

Study Protocol

Two groups were set in this study based on injecting saline (0.5 mL per GP) or the selective $Na_v1.8$ blocker A-803467 (1 μmol/0.5 mL per GP) into both ARGP and SLGP. After drug administrating, RAP was delivered at the LAA (20 Hz, 10 diastolic threshold) for 6 hours. At the end of RAP, targeted parameters-effective refractory period (ERP) and window of vulnerability (WOV) were evaluated as previously described.[16,18] Briefly, we measured ERP by using S1-S1 programmed stimulating at 330 ms interval and S1-S2 interval from 150 ms with decrementing at 10 and 1 ms when approaching the refractory period (S1:S2=8:1, 10 TH). To delineate AF inducibility, WOV was calculated as the difference between the longest and the shortest S1-S2 interval. ERP dispersion was assessed as the coefficient of variation of ERP at all 8 recording sites. AF was defined as irregular atrial rates related with irregular atrioventricular conduction at more than 500 bpm lasting at least 5 seconds. AF cycle length was measured as the averaged first 10 fibrillation waves at the onset of AF. The number of AF episodes and averaged AF duration were also recorded at each group. Representative traces in the electrophysiological study before and after administrating A-803467 at GPs are shown in Figure 1C and Figure 1D.

Tissue Preparation and Immunofluorescence

Cardiac ganglia were quickly obtained from 3 canine heart fat pads located at the atria posterior wall. After that, they were placed into normal Krebs solution in ice, dissected under a stereomicroscope, and put into liquid nitrogen for flash freezing. Cryosections from embedded ganglia tissue were fixed in 4% paraformaldehyde for 10 minutes, permeabilized in 0.3% Triton X-100 in PBS for 15 minutes, and all blocked in 5% donkey serum for 30 minutes at room temperature. Tissue sections were incubated at 4°C overnight with primary antibody specific for rabbit polyclonal anti-Nav1.8 (Alomone Labs, Jerusalem, Israel), rabbit polyclonal anti-Nav1.5 (Alomone Labs, Jerusalem, Israel), goat polyclonal anti-PGP9.5 (Abcam, Cambridge, MA), goat polyclonal anti-choline acetyltransferase (ChAT, CHEMICON International, Temecula, Canada), and mouse monoclonal anti-tyrosine hydroxylase (TH, Alpha Diagnostic International, San Antonio, TX). Alexa 488-conjugated secondary antibody was then added according to a different source of primary antibody and incubated for 90 minutes at room temperature. Stained samples were

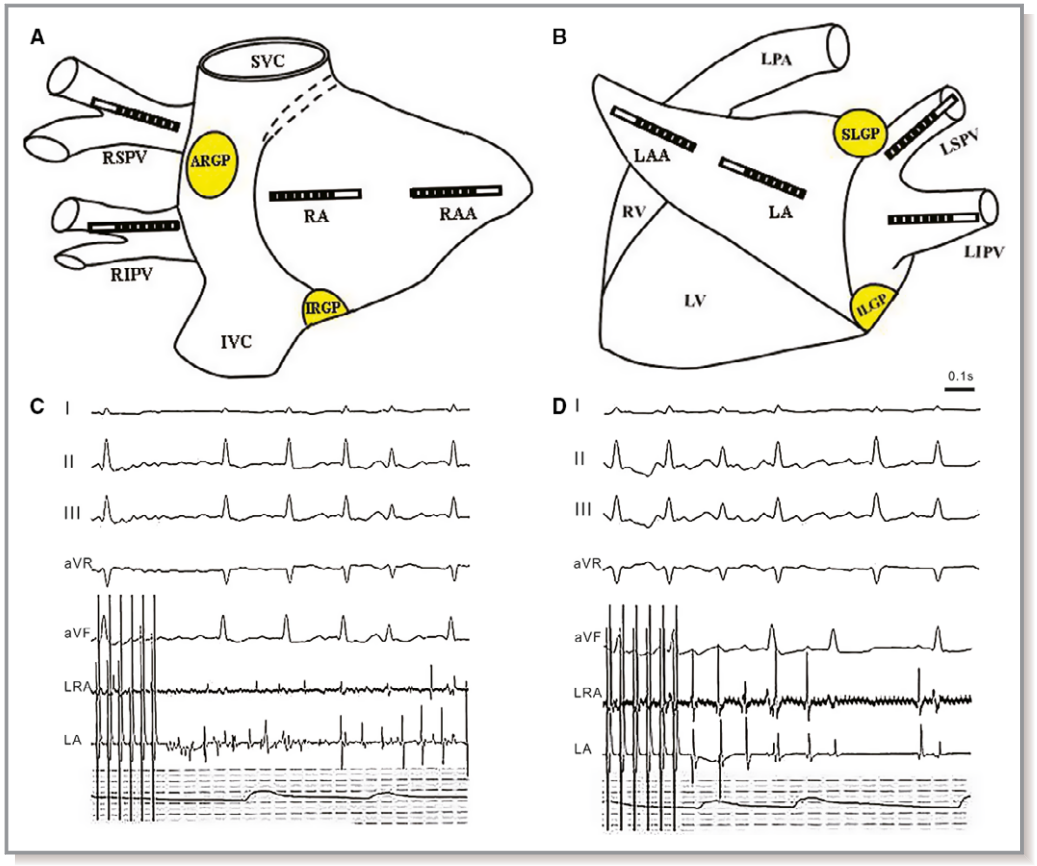

Figure 1. Schematic catheter positions in the atria and pulmonary veins and representative traces. A, Left thoracotomy approach. B, Right thoracotomy approach. Electrode catheters were sutured to the left superior pulmonary vein (LSPV), left inferior pulmonary vein (LIPV), left atrium (LA), left atrial appendage (LAA), right superior pulmonary vein (RSPV), right inferior pulmonary vein (RIPV), right atrium (RA), and right atrial appendage (RAA). ARGP indicates anterior right ganglionated plexi; ILGP, inferior left ganglionated plexi; IRGP, inferior right ganglionated plexi; IVC, inferior vena cava; LPA, left pulmonary artery; LV, left ventricle; SLGP, superior left ganglionated plexi; SVC, superior vena cava; RV, right ventricle. C and D, Representative traces in the electrophysiological study before and after administrating A-803467 at ganglionated plexus.

visualized under an Olympus FluoView laser scanning confocal microscope (Olympus, Orangeburg, NY). Images were acquired with the FluoView acquisition program and analyzed by ImageJ software.

Coexpression of NaV1.5 and NaV1.8 and Patch Clamp Study

TSA-201 cells transfected with *SCN5A*, *SCN10A,* and *SCN3B* plasmids were used for patch clamp study. A plasmid encoding EGFP was used to identify transfected cells. Briefly, transient transfection using FuGENE 6 (Roche Diagnostics, Indianapolis, Indiana) was carried out with *SCN10A*, *SCN5A,* and *SCN3B* with a molar ratio of 5:5:1 (for a total of 2.25 μg of DNA). The cells were grown in GIBCO DMEM medium (No. 10566, Gibcowith FBS [No. 16000] and antibiotics [No. 15140], Life Technologies) on polylysine-coated 35 mm culture dishes (Cell+, Sarstedt, Newton, NC). Cells were placed in a 5% CO_2 incubator at 37°C for 24 to 48 hours prior to patch clamp study.

Membrane currents were measured using whole-cell patch clamp techniques. All recordings were obtained at room temperature (20–22°C) using an Axopatch 200B amplifier equipped with a CV-201A head stage (Axon Instruments Inc./ Molecular Devices, Union City, CA). Currents were filtered with a 4-pole Bessel filter at 5 kHz and digitized at 50 kHz. Series resistance was compensated at around 80% to assure that the command potential was reached within microseconds with a voltage error <2 mV. Cells were allowed to stabilize for 10 minutes after establishment of the whole-cell configuration before current was measured. Macroscopic whole-cell Na+ current was recorded by using bath solution perfusion containing (in mmol/L) 140 NaCl, 4 KCl, 1.8 $CaCl_2$, 1 $MgCl_2$, 10 HEPES, and 10 Dextrose (pH 7.35 with NaOH). Osmolarity was adjusted to 310 mmol/kg with sucrose. Patch pipettes were fabricated from 1.5 mm OD borosilicate glass capillaries

(Fisher Scientific Inc, Hampton, NH). They were pulled using a gravity puller (Model PP-830, Narishige International USA, Inc, East Meadow, NY) to obtain resistances between 0.8 and 2.2 MΩ when filled with a pipette solution containing (in mmol/L) 10 NaF, 105 CsF, 20 CsCl, 2 EGTA, and 10 HEPES with a pH of 7.35 adjusted with CsOH and an osmolality of 300 mmol/kg with sucrose.

Specific voltage-clamp protocols assessing channel activation and fast inactivation were used, as depicted in the figure insets. Cardiac sodium channel current (I_{Na}) was elicited by depolarizing pulses ranging from −90 to +40 mV in 5 mV increments with a holding potential of −120 mV. Peak currents ($I_{Na,P}$) were measured and I_{Na} densities (pA/pF) were attained by dividing the obtained cell capacitance. Activation properties were determined from I/V relationships by normalizing $I_{Na,P}$ to driving force and maximal I_{Na}, and plotting normalized conductance versus V_m. Voltage dependence of steady-state inactivation was obtained by plotting the normalized $I_{Na,P}$ (40-ms test pulse to −0 mV after a 1000-ms conditioning pulse from −140 to −10 mV with the holding potential of −120 mV) versus V_m. The steady-state channel availability and inactivation curves were fitted to the Boltzmann equation, $I/I_{max}=1/(1+\exp((V-V_{1/2})/\kappa))$, to determine the membrane potential for half-maximal activation/inactivation ($V_{1/2}$) and the slope factor (κ). Pulses for recovery from inactivation were of 100 ms duration for P1 and 50 ms for P2. The peak current elicited during the second pulse was normalized to the value obtained during the initial test pulse. It was analyzed by fitting data to a double exponential function: $I(t)/I_{max}=Af\cdot(1-\exp(-t/\tau_f))+As\cdot(1-\exp(-t/\tau_s))$, where Af and As are the fractions of fast and slow inactivating components, respectively, and τ_f and τ_s are their time constants.

All data acquisition and analysis were performed using pCLAMP version 9.2 (Molecular Devices, Sunnyvale, CA), Excel (Microsoft, Redmond, WA), and Origin 7.5 (MicroCal Software, GE Healthcare, Pittsburgh, PA).

Statistics

All continuous data are presented as mean±standard error (SE). Student *t* test was used to analyze those continuous data. For nonparametric data, Fisher exact test was used to compare 2 groups. Statistical significance was selected at a 2-sided *P* value of 0.05.

Results

$Na_v1.8$ and $Na_v1.5$ Expression in Canine Cardiac Ganglia

As shown in Figure 2, adult canine cardiac ganglias were partially dissected and labeled by neuron marker PGP9.5, TH,

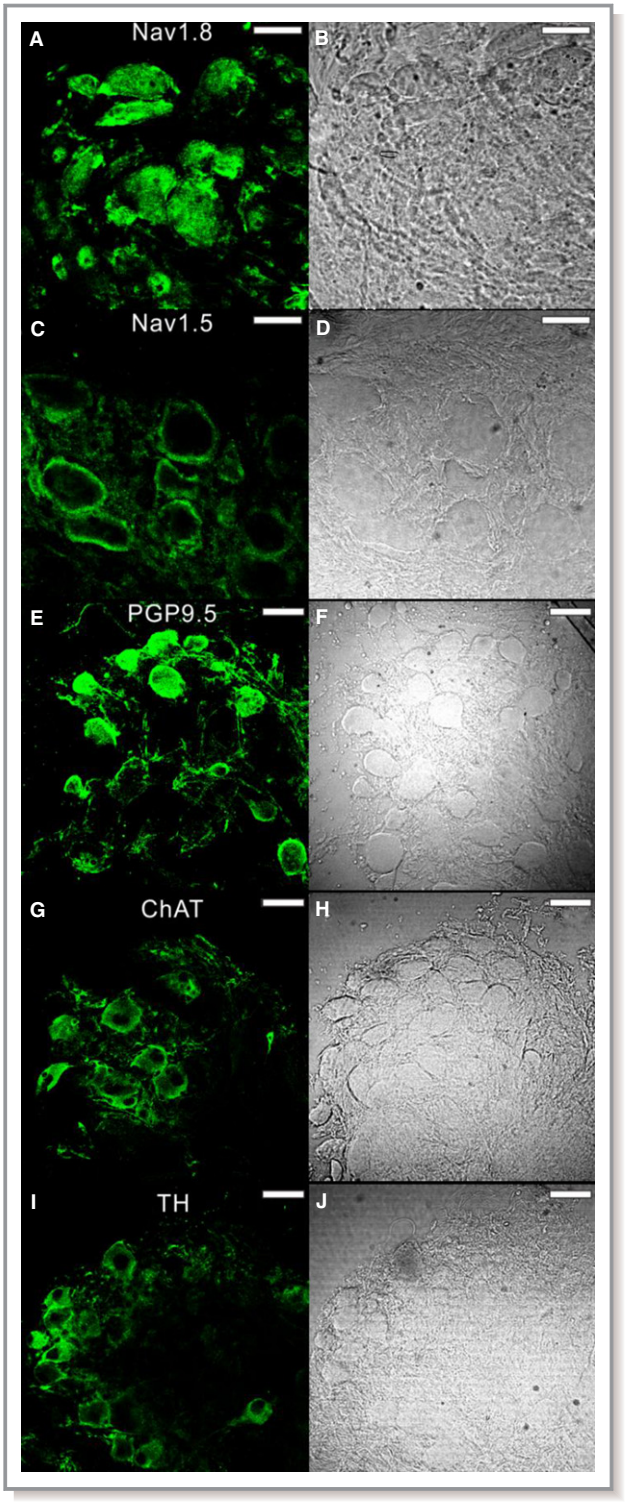

Figure 2. Immunochemical study of Nav1.8, Nav1.5, PGP9.5, anti-choline acetyltransferase (ChAT), and anti-tyrosine hydroxylase (TH) in partial dissected intracardiac ganglia. Protein expression of Nav1.8 (A and B), Nav1.5 (C and D), PGP9.5 (E and F), ChAT (G and H), and TH (I and J) present in intracardiac ganglia. Images on the left side show fluorescein isothiocyanate green fluorescence. Images on the right side show nonstained components of the ganglia. Calibration bars in (A through D) are 20 μm and in (E through J) are 50 μm.

and ChAT. Both adrenergic and cholinergic neurons can be found in those ganglias (Figure 2G through 2J). Staining of $Na_v1.8$ and $Na_v1.5$ separately proved their expression on canine GP (Figure 2A through 2D). The 2 sodium channels can be observed in both membrane and cytoplasm under high magnification and no significant differences were found in regard to the channel distribution in adrenergic and cholinergic neurons (data not shown).

Effect of A-803467 on ERP and AF Inducibility in GPs

Representative traces in the electrophysiological study before and after administrating A-803467 at GPs are displayed in Figure 1C and Figure 1D. Mean ERP at baseline between the control and A-803467 groups was similar at all 8 recording sites (97.98±6.86 versus 97.95±7.30 ms, $P>0.05$, 10x threshold). After administrating saline or A-803467, respectively, to the 2 groups at ARGP and SLGP, rapid pacing was implemented at LAA. The ERPs were reevaluated at the end of 6-hour RAP by the same protocol. Compared with the control group, the shortening of ERP at all PV and atrial sites was suppressed in the A-803467 group (Figure 3, $P<0.05$).

ERP dispersion and cumulative WOV (ΣWOV) were calculated and AF inducibility was compared between the 2 groups before and after RAP. No baseline differences at ERP dispersion or ΣWOV were found between the 2 groups before RAP (ERP dispersion: 0.15±0.15 versus 0.14±0.13 ms; ΣWOV: 19.30±3.51 versus 18.13±2.34 ms; $P>0.05$ [Figure 4D and 4E]). After 6-hour RAP, both ERP dispersion and ΣWOV were significantly increased in the control group. However, injecting A-803467 at GPs attenuated the increase in ERP dispersion and ΣWOV apparently at all sites, underlying the decrease in AF inducibility (Figure 4D and 4E, ERP dispersion: 0.29±0.15 versus 0.15±0.13, ΣWOV: 180.70±20.47 versus 21.64±5.84 ms; $P<0.01$).

After 6-hour RAP, spontaneous AF occurred in 7 dogs in the control group (N=8), whereas it occurred in only 2 dogs in the A-803467 group (N=8), with an incidence of 87.50% versus 25.0% (Figure 4C). In addition, administrating A-803467 can also shorten AF duration and prolong AF cycle length in contrast to that in the control group (AF duration: 47.05±10.45 seconds versus 18.18±6.59 seconds, $P<0.05$; AF cycle length: 79.21±1.24 versus 129.77±17.41 ms, $P<0.05$ [Figure 4A and 4B]).

Characterization of A-803467 at 100 nmol/L on *SCN5A-SCN10A-SCN3B* Cotransfected TSA201 Cells

Previous reports have shown the abundant expression of β3 subunit (*SCN3B*) in dorsal root ganglion neurons and have

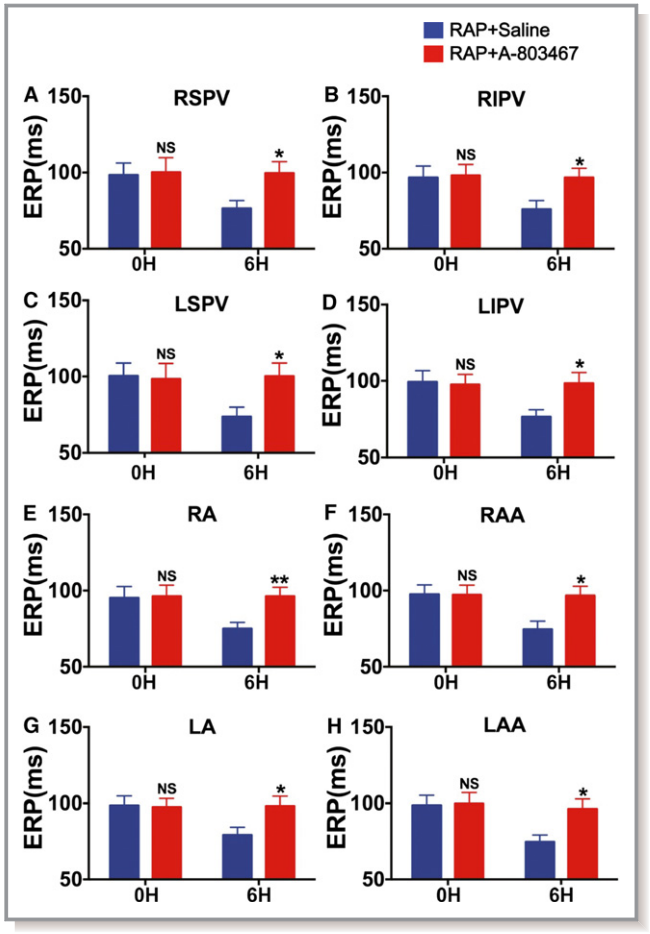

Figure 3. Mean effective refractory period (ERP) values are shown at all 8 recording sites in 2 study groups. Rapid atrial pacing (RAP)+saline (N=8) and RAP+A-803467 (N=8). At all sites (A through H), mean ERP decreased significantly after 6 hours of RAP (not significant [NS], $P>0.05$; *$P<0.05$, vs RAP+saline at the same time point). LA indicates left atrium; LIPV, left inferior pulmonary vein; LSPV, left superior pulmonary vein; RA, right atrium; RAA, right atrial appendage; RIPV, right inferior pulmonary vein; RSPV, right superior pulmonary vein.

emphasized that the β3 subunit can promote the trafficking of $Na_v1.8$ and help its expression on membrane in comparison to other β subunits without changing gating properties.[19,20] Based on that, *SCN5A-SCN10A-SCN3B*-WT was cotransfected into TSA201 cells in the present study to depict the electrophysiological characteristics of the sodium channel composed of *SCN5A-SCN10A* under 100 nmol/L A-803467. A significant reduction was shown with 100 nmol/L A-803467 on the current-voltage relationship, whereas no difference was found at the same concentration with *SCN5A-SCN3B*-WT (Figure 5A). Furthermore, electrophysiological characteristic properties were implemented on the cells transfected with *SCN5A-SCN10A-SCN3B*-WT. Other and our previous results have reported the extremely low current density when *SCN10A* was transfected into TSA201 cells,

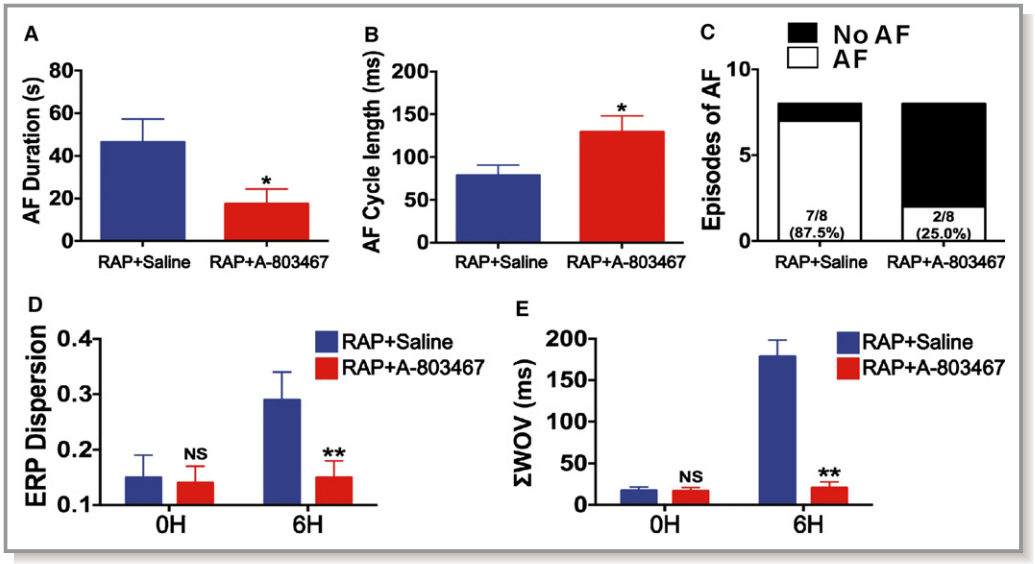

Figure 4. Changes in programmed stimulating parameters in 2 groups before and after 6-hour rapid atrial pacing (RAP). A through C, atrial fibrillation (AF) duration, cycle length, and episodes after 6-hour RAP. D and E, Effective refractory period (ERP) dispersion and cumulative window of vulnerability (ΣWOV) changes at baseline (0 hour) and after 6-hour RAP. Not significant (NS), $P>0.05$; *$P<0.05$; **$P<0.01$ vs RAP+saline at the same time point. In RAP+saline, RAP resulted in significant decreases in ERP and increases in ERP dispersion, ΣWOV, and AF inducibility. In RAP+A-803467, however, these changes were significantly attenuated.

with or without sodium β subunit.[9,21] Hence, the blocking effect of A-803467 was not performed on *SCN10A-SCN3B*-WT transfected TSA201 cells.

A-803467 reduced maximum $I_{Na,P}$ by 45% ($I_{Na,P}$, from −758.77±173.48 to −414.75±92.44 pA/pF, n=8; $P<0.01$) with similar I-V curve ($I_{Na,P}$ amplitudes at −35 mV) between the control and A-803467 groups (Figure 5B and 5C). In addition, $I_{Na,L}$ was measured under 100 nmol/L A-803467 between 295 and 300 ms by the test pulse at −20 mV from HP of −120 mV at the rate of 0.2 Hz (Figure 5D). Relative $I_{Na,L}$ (percentage of $I_{Na,P}$) decreased from 0.52% to 0.20%. The inhibitions of $I_{Na,P}$ and $I_{Na,L}$ under the same protocol were also compared. Both the $I_{Na,P}$ and $I_{Na,L}$ in control conditions were regarded as 100%. As presented in Figure 5E, after applying A-803467, a more pronounced inhibition with $I_{Na,L}$ than $I_{Na,P}$ was shown: $I_{Na,P}$ was decreased 42.02±3.88% and $I_{Na,L}$ was decreased 68.57±5.86% (n=8 for each group, $P=0.02$).

Figure 6A shows a hyperpolarized shift of steady-state inactivation by the influence of 100 nmol/L A-803467 under a 100 ms prepulse to various potentials in 10 mV step followed by a 20 ms test pulse to 0 mV. A-803467 caused a prominent negative shift of the $V_{1/2}$ of inactivation from −83.76±2.38 to −95.77±3.20 mV (n=12, $P<0.05$), predicting less availability of channels open at physiological resting potential or sustained depolarization with the drug. As shown in Figure 6B and the Table, there was no significant difference in steady-state activation before and after applying the drug ($V_{1/2}$: −49.52±2.74 and −51.95±1.38 mV, n=12 [$P=0.44$]; κ: −5.21±0.48 and −5.78±0.24, n=12 [$P=0.30$]).

Recovery from inactivation was also assessed before and after drug administration by using a standard 2-pulse protocol: first test −10 mV for 100 ms then recovering at −120 mV for a various duration before a second pulse at −10 mV for 50 ms. As displayed in the representative traces (Figure 6C), A-803467 inhibited the process of recovery from inactivation. A 2-exponential equation was used for fitting, and time constants were compared. Both the fast (τ_f) and slow (τ_s) time constants were much slower in the presence of 100 nmol/L A-803467 (τ_f: 2.87±0.38 versus 6.46±0.58, n=14 [$P<0.01$]; τ_s: 20.51±0.61 versus 64.37±15.47, n=14 [$P=0.01$], Figure 6D, Table).

For further study, use-dependent block (UDB) was investigated in the absence and presence of A-803467 via a series of 40 pulses to −20 mV from −120 mV holding potential at the rate of 1, 2, and 10 Hz. The proportion of the 40th and first current amplitudes was compared between control and drug conditions under these 3 different frequencies. For the control group, the proportions of $I_{Na,P}$ were 97.38%, 95.80%, and 93.89%, and for the drug were 95.95%, 89.81%, and 83.96%, at the rate of 1, 2, and 10 Hz, respectively (Figure 7B). The inhibition effect of A-803467 was more evident at faster rates (reduction at 1/2/10 Hz was 3.68%/6.06%/12.78%, N=9 [$P<0.01$]). Figure 7A shows the exemplified traces at 10 Hz. Both traces of the 2 conditions were

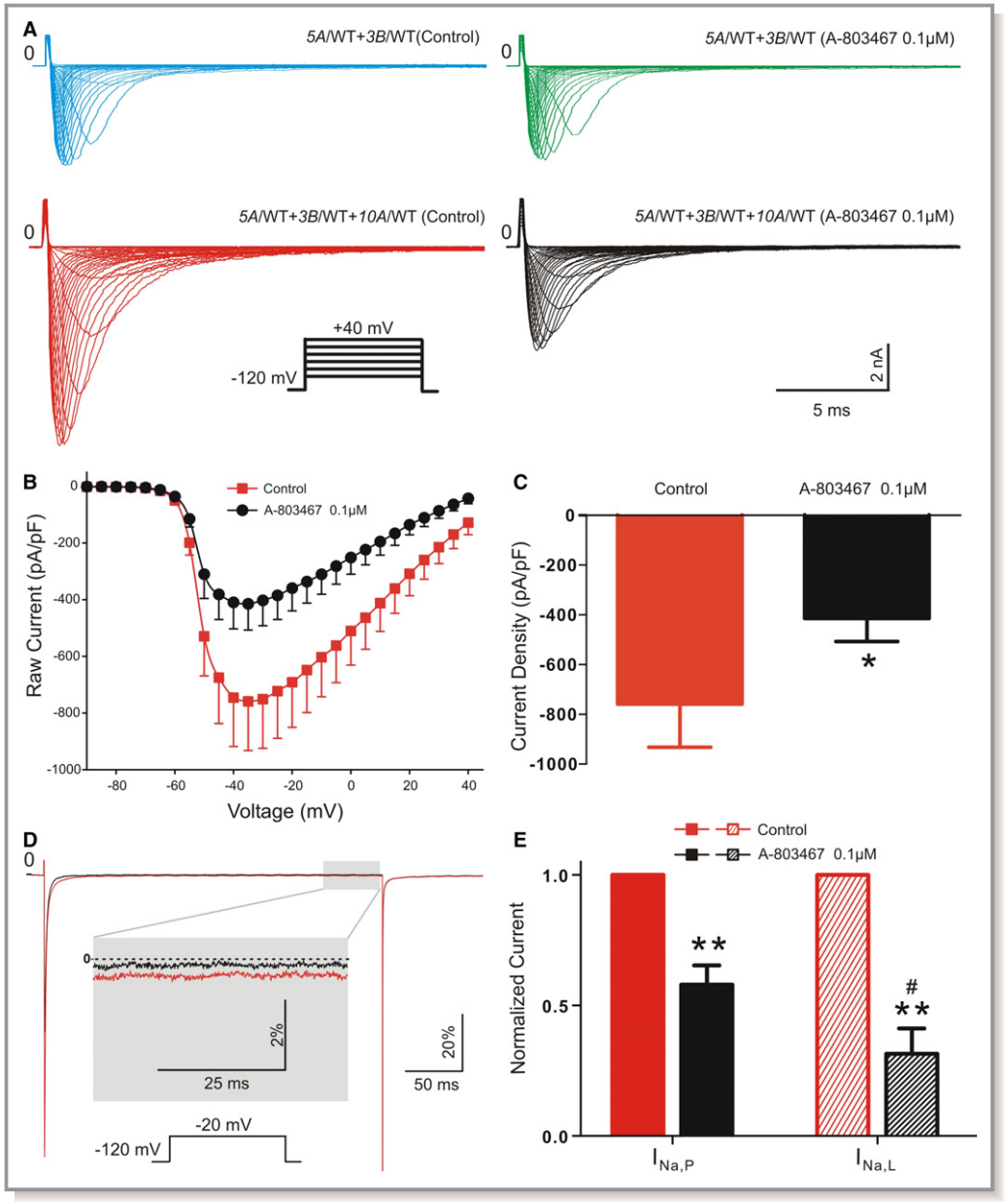

Figure 5. Electrophysiological effect of A-803467 at 100 nmol/L on *SCN10A-SCN5A-SCN3B* coexpressed TSA201 cells. A, Representative $I_{Na,P}$ traces in *SCN5A*-WT+*SCN3B*-WT transfected cells, and *SCN10A*-WT+*SCN5A*-WT+*SCN3B*-WT cotransfected cells with and without 100 nmol/L A-803467 separately. B and C, Current-voltage relationship and $I_{Na,P}$ current density depicting $I_{Na,P}$ recording from coexpression of *SCN10A*-WT+*SCN5A*-WT+*SCN3B*-WT before and after perfusing with 100 nmol/L A-803467. **P*<0.05 compared 2 groups. D, Representative traces and blocking effect of 100 nmol/L A-803467 on $I_{Na,L}$, as the percentage of $I_{Na,P}$. **P*<0.05 compared 2 groups. E, Comparison of normalized current of $I_{Na,P}$ and $I_{Na,L}$ between the control and A-803467 100 nmol/L groups.

positioned at the same scale so that the noticeable reduction under drug influence was more obvious in comparison. Together with the inhibition of recovery from inactivation, A-803467 may interact with the inactivated state of these sodium channels. In addition, a frequency-dependent reduction was also observed in $I_{Na,L}$. Figure 7D shows the relative current proportion of $I_{Na,L}$ at −20 mV in the rate of 2 Hz. In the control condition, there was more inhibition of $I_{Na,L}$ than that in $I_{Na,P}$, with 68.99±3.67% versus 95.80±1.75% remaining after the 40th pulse. When the drug was applied, the value of $I_{Na,L}$ and $I_{Na,P}$ decreased to 60.64±3.98% and 89.43±2.06% (reduced rate of $I_{Na,L}$ versus $I_{Na,P}$; 12±04% versus 6±2%, N=8 for each group [*P*=0.04]). The result indicates preferential UDB of A-803467 on $I_{Na,L}$ than $I_{Na,P}$.

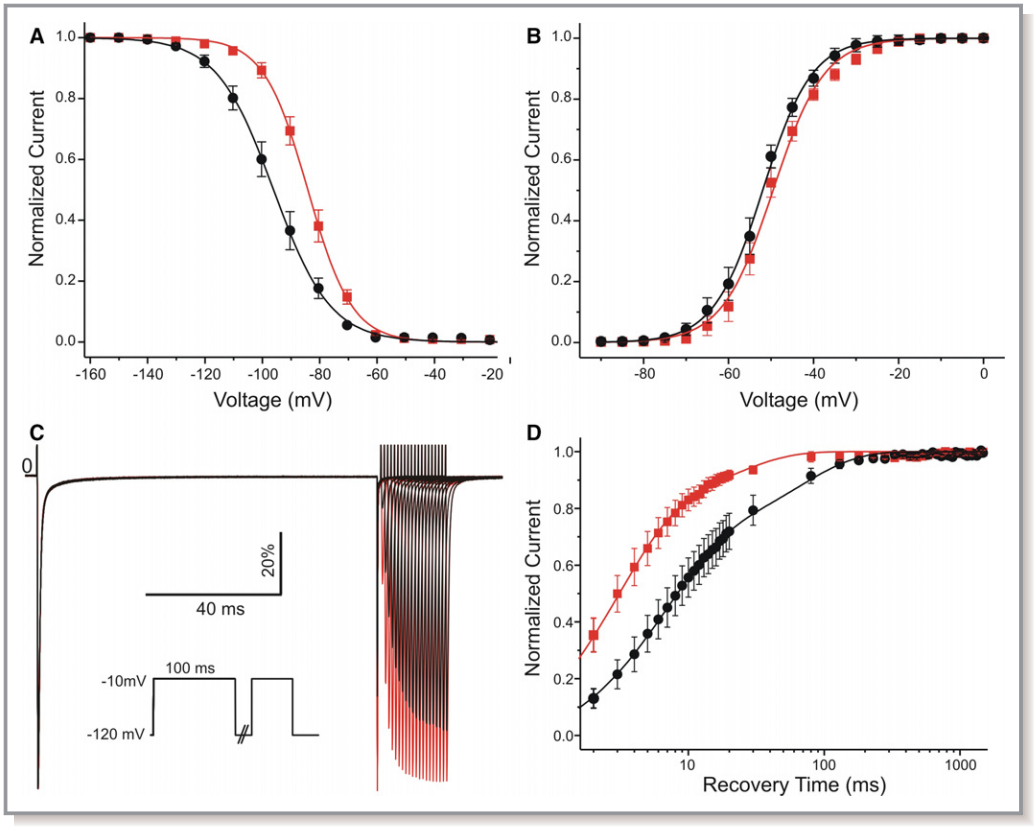

Figure 6. Effect of A-803467 at 100 nmol/L on the kinetics of *SCN10A-SCN5A-SCN3B* coexpressed TSA201 cells. A, Steady-state inactivation curves for the control and A-803467 groups. Administrating A-803467 can hyperpolarize the inactivation curve by ≈10 mV ($P<0.05$). B, Steady-state inactivation curves for the control and A-803467 groups. Boltzmann analysis showed that the slope factor (κ) and the half-activation potential did not differ significantly between groups. C, Representative recovery traces elicited from −120 mV holding potential to 100 ms inactivating pulse followed by variable duration (1–1480 ms) to allow the recovery with and without A-803467. D, Effects of A-803467 on recovery from inactivation between the 2 groups by 2 exponential fitting. Both fast and slow time constants were increased after applying A-803467.

Discussion

In this study, we demonstrate that, in a canine acute AF model, pharmacological inhibition of $Na_v1.8$ on GP can prevent electrical remodeling at PV and atrial myocardium and further reduce the incidence of paroxysmal AF. Sodium channel properties were obviously affected by the $Na_v1.8$ blocker when *SCN5A-SCN10A-SCN3B*-WT coexpressed in vitro, which indicates a possible underlying mechanism of our animal model results. The transfected sodium channel complex with 100 nmol/L A-803467 displayed decreased I_{Na}, and faster inactivation, slower recovery, and stronger UDB on both $I_{Na,P}$ and $I_{Na,L}$ in contrast to the characteristics before the drug.

Table. Effects of A-803467 on the Kinetics Gating Parameters in *SCN10A-SCN5A-SCN3B* Coexpression TSA201 Cells

	Inactivation			Activation			Recovery		
SCN5A-SCN10A-SCN3B	$V_{1/2}$, mV	κ, mV	No.	$V_{1/2}$, mV	κ, mV	No.	τ_f, ms	τ_s, ms	No.
Control	−83.76±2.38	7.70±0.39	12	−49.52±2.74	5.21±0.48	12	2.87±0.38	20.51±5.61	14
A-803467, 100 nmol/L	95.77±3.20*	8.94±0.48*	12	−51.95±1.38	5.78±0.24	12	6.46±0.58*	64.37±15.47*	14

Parameters of inactivation and activation were calculated from the Boltzmann function. $V_{1/2}$ is the voltage for half-maximal availability or activation and κ is the slope factor. Parameters of recovery were fitted to a double exponential function.
*$P<0.05$ vs control group. Data are from Figure 6 and are reported as mean±SEM.

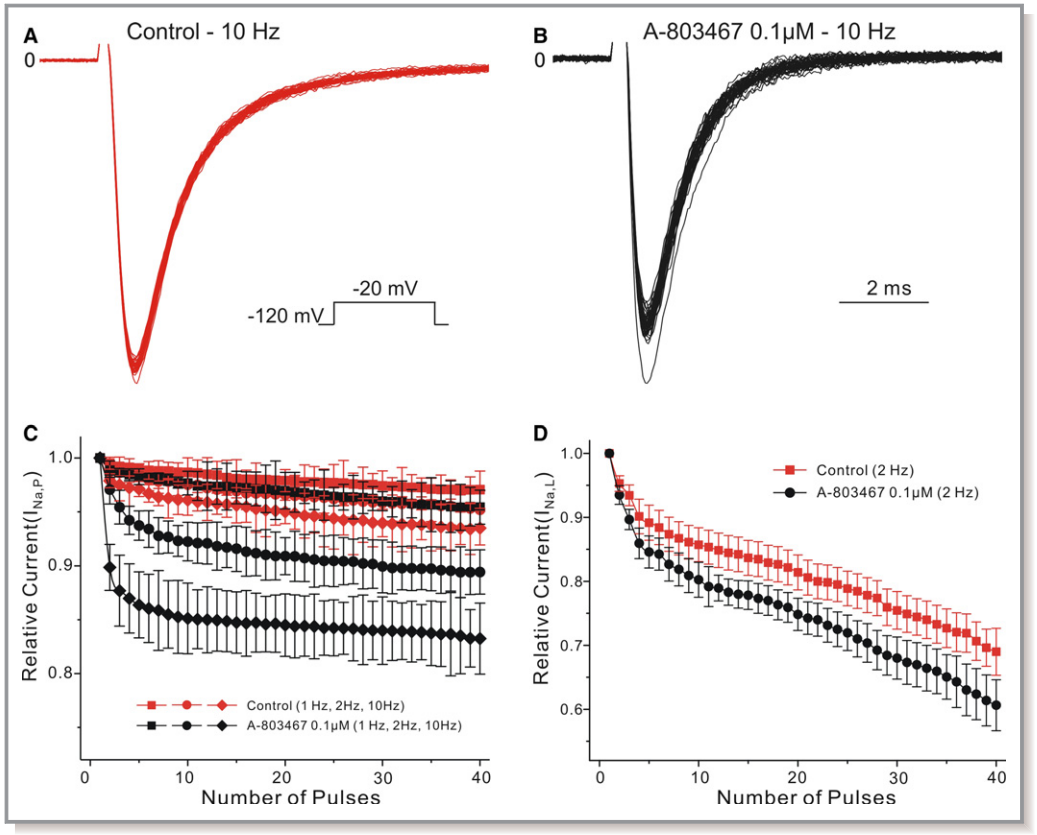

Figure 7. Use-dependent block (UDB) in the control and A-803467 100 nmol/L groups. A and B, Current recordings between the 2 groups. Pulse duration was 20 ms, and the holding potential was −120 mV and given at a rate of 0.1 seconds (10 Hz). C, UDB of $I_{Na,P}$ in the control and A-803467 groups at 1, 2, and 10 Hz. D, UDB of $I_{Na,L}$ in the control and A-803467 groups at 2 Hz.

Focal firing and vulnerable substrate are requisite for AF initiation and maintenance. One study by Nattel and colleagues[22,23] verified that GPs played a vital role in the experimental AF related to atrial tachycardia remodeling. Compared with small effect on AF vulnerability by PV isolation, GP ablation could reduce AF vulnerability and attenuate AF maintenance by prolonging ERP, reducing AF duration and dominant frequency of fibrillatory activity. In addition, GP stimulation increases vagal and sympathetic tone, which induces early afterrepolarization formation, enhances Ca^{2+} transient facilitating trigger activity, and shortens action potential duration, especially at PV myocardium, increasing heterogeneous repolarization and prompting substrate and re-entry within atria.[3,24,25] RAP can shorten ERP and increase ERP dispersion and ΣWOV, which were all reversed after GP ablation. Implementing GP ablation or autonomic blockers (atropine or propranolol) followed by RAP can prevent induced spontaneous AF and atrial electrical remodeling.[26,27] In our study, administrating A-803467 can effectively attenuate ERP shortening and suppress increased ERP dispersion and ΣWOV, indicating a pharmacological denervation effect by this selective $Na_v1.8$ blocker. Voltage-gated sodium channels are responsible for generating and propagating action potentials and are critical in neuronal firing and excitability. Therefore, our results suggest that blocking $Na_v1.8$ can decrease GP firing, inhibit its activity, and prevent the initiation and maintenance of RAP-induced AF. Similar findings were observed by Qi and colleagues.[15] They applied a different AF-induced model by vagus nerve stimulation (VNS) to evaluate cardiac conduction and AF inducibility after injecting A-803467 on ARGP and inferior right ganglionated plexi at the same concentration. They concluded that blockade of $Na_v1.8$ could suppress the effect of VNS on sinus rate, PR interval, and ventricular rate when AF occurred during VNS. The values of ERP in the control group after GP injection were lower than ours probably because of VNS. Previous study demonstrated that ARGP and SLGP in the intrinsic cardiac autonomic nerve system collected the nerve from both vagosympathetic trunk as integration center, and either ARGP or SLGP ablation could eliminated ERP shortening during vagosympathetic trunk stimulation. Ablating ARGP could also eliminate AF inducibility during high-frequency atrial pacing. It identified that ARGP and SLGP are the main connections in the neural pathway to control intrinsic

autonomic activity in AF.[28] Therefore, ablation (drug denervation) of ARGP and SLGP could be sufficient to show the effect of AF prevention. In the present study, we chosen ARGP and SLGP for injection and applied 6-hour RAP after injection to assess the effect of blocking $Na_v1.8$ on acute AF directly. Decreased ERPs were found in all atrium and pulmonary recording sites, which were suppressed when A-803467 were administrated in advance. This could suggest that blocking $Na_v1.8$ could avoid functional substrate forming in PV myocardium, probably as a result of inhibiting GP function and atrial electrical remodeling. Although we could not deny the fact that sodium pentobarbital has been reported vagolytic and may increase the ERP value when applying,[29,30] the effect of A-803467 on ERP in the present study is still established, since both groups were treated equally with the anesthetic to eliminate bias between groups, and the minimum dosage was used to reduce the possibility of unnecessary influence, as in our previously published studies.[18,26,31,32]

Scherlag et al[33] injected lidocaine into GPs, leading to the loss of AF inducibility in 6 of 7 dogs. Our results displayed an apparent inhibition with 25.0% AF incidence when applying A-803467, compared with 87.5% in the control group (odds ratio=21.00). As a class I antiarrhythmic drug and local anesthetic, lidocaine proved to have a pronounced effect in inhibiting $Na_v1.8$ current, enhancing UDB, and regulating gating properties.[34] A-803467, as a selective $Na_v1.8$ blocker, is used in alleviating $Na_v1.8$-involved neuropathic pain. In recombinant HEK293 cells, A-803467 was blocked human $Na_v1.8$ (IC_{50}=8 nmol/L), and was >100-fold selective versus human Nav1.2, Nav1.3, Nav1.5, and Nav1.7 (IC_{50} >1 μmol/L).[35] In the present study, TSA201 cells were transfected with *SCN5A-SCN10A-SCN3B*, A-803467 at 100 nmol/L potently inhibited $I_{Na,P}$ by 42.02%, and it suppressed more in $I_{Na,L}$ by 68.57%. Gating properties were also changed under A-803467 with hyperpolarized steady-state inactivation and delayed recovery from inactivation. Interestingly, the left-shifted steady-state inactivation was quite consistent with the effect of A-803467 in isolated mouse intracardiac neurons delineated by Verkerk et al.[36] Like other sodium channel blockers, our results support that A-803467 might block sodium channels in an inactivated state and the number of trapped inactivated sodium channels might be increased during repeated stimulation. Obvious delay of recovery was displayed as 2 times slower in τ_f and more than 3 times in τ_s. As expected, UDB was also observed under A-803467. Inhibition in $I_{Na,P}$ could reduce neuronal excitability, which might explain the pharmacological denervation effect. The changes in gating properties, together with UDB, indicate reduced availability of the sodium channel under sustained depolarization or repetitive stimulation, especially in a RAP-induced AF model.

In the present study, we utilized the *SCN5A-SCN10A-SCN3B* cotransfected model to analyze the effect of A-803467 on sodium current and gating properties to provide a possible explanation for the results we found in animal experiments. Compared with *SCN5A-SCN3B* transfected TSA-201 cells, the current density was significantly increased and was sensitive to A-803467 when *SCN10A* were added together with *SCN5A-SCN3B*. Since others' and our studies have reported the extremely low current density in *SCN10A-SCN3B* transfected cell lines,[9,21] it is reasonable to deduce that the increased current is not an arithmetic addition of current component produced by *SCN10A*. It implies that *SCN10A* might interact with *SCN5A* as a new sodium complex (Figure 8), and A-803467 could have an effect on *SCN10A-SCN5A* complex, as indicated in our patch clamp study. Although the complicated protein network of this new complex needs to be further explored, this model cells might be help us to understand the electrophysiological role of $Na_v1.8$ in arrhythmias.

Many association studies have discovered the intensive relationship between *SCN10A* variants and AF phenotype or incidence. In addition to the significant effect on GP, $Na_v1.8$ might directly influence the electrophysiological characteristics of cardiac tissue with suppressed trigger activity and reduced substrate during AF (Figure 8). The decreased current in $I_{Na,P}$ by A-803467 might prolong ERP in atrium by virtue of postrepolarization refractoriness and reduce excitability at the fast rate due to UDB. The prolonged ERP might also prevent the formation of functional substrate during acute AF. Decreased $I_{Na,P}$ might also cause conduction block to break the reentrant circuit. The significantly reduced $I_{Na,L}$ seen in our study might suppress the incidence of early afterrepolarization during AF. Yang et al[21] also showed that 30 nmol/L A-803467 can remarkably reduce $I_{Na,L}$ in mouse and rabbit myocytes with less effect on $I_{Na,P}$. In addition, the inhibition of sodium channel by A-803467 can reduce Na^+ in myocytes during repolarization, which may prevent the Ca^{2+} loading to inhibit delay after repolarization. The suppressed trigger activity and reduced substrate could also be potential mechanisms for inhibiting AF initiation and maintenance.

Genome-wide association studies have opened up a new horizon in understanding cardiac electrophysiology. Several independent loci of *SCN10A* were indicated to increase PR and/or QRS intervals, which were regarded as intermediate phenotypes, suggesting the risk of conduction disease and arrhythmia susceptibility.[37,38] There is an increased number of studies that focus on the relationship of *SCN10A*/$Na_v1.8$ with cardiac diseases. In spite of several disputes such as the expression of $Na_v1.8$ in the heart,[36,39] $Na_v1.8$ is critical in cardiac electrophysiology. Our previous study first reported 17 putative pathogenic *SCN10A* variants in 25 of 150 Brugada syndrome probands with a positive proband yield of 16.7%,

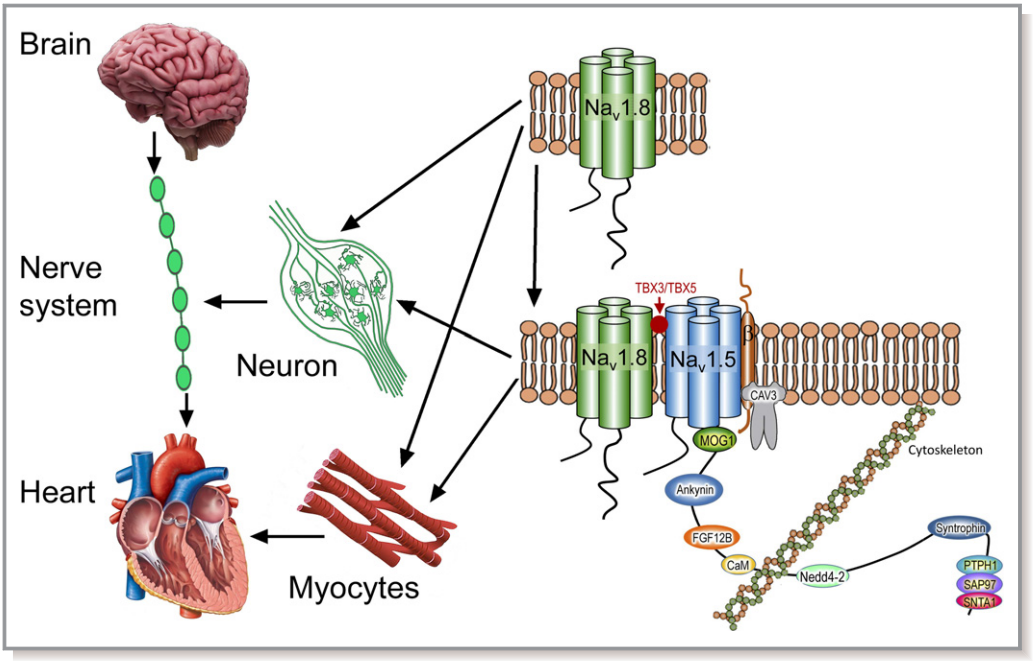

Figure 8. Schematic summary of potential pathways of $Na_v1.8$ for regulating cardiac function. $Na_v1.8$ has been proved to exist in both autonomic ganglia and cardiac tissue. Our previous results demonstrated the association between $Na_v1.8$ and $Na_v1.5$ at the protein level when expressed separately ex vivo.[9] In the present study, A-803467 have apparent effects on current density and gating kinetics when coexpressed sodium complex of *SCN10A-SCN5A-SCN3B,* which indirectly show the functional interaction between the 2 alpha sodium units. The detailed components of the complicated sodium complex in the cytoplasm need to be specifically explored. This sodium complex could exert its role through ganglionated plexus and/or cardiac myocytes. Given their proximity to one another, *SCN5A* and *SCN10A* may be subject to common regulatory mechanisms, such as transcriptional control by *TBX3* and *TBX5*.

approaching our historical yield of 20.1% for *SCN5A*. Subsequent studies from others also emphasize the importance of *SCN10A* in both rare and common variants in Brugada syndrome.[9] One recent study concluded that rs6795970 might be associated with cardiac conduction abnormalities in patients with hypertrophic cardiomyopathy.[40] Therefore, it has come a long way as the "new cardiac sodium channel," and the exact roles of $Na_v1.8$ in arrhythmia still have a long way to go. It can be considered as a novel target in understanding cardiac electrophysiology, and its selective blocker or other relative drug might be promising in *SCN10A*-related arrhythmias.

Study Limitations

We did not record GP activity directly in our RAP-induced canine AF model in the absence or presence of A-803467. However, previous studies have demonstrated that blocking GP activity can inhibit RAP-induced atrial electrical remodeling and AF inducibility. After we administrated A-803467 in GPs, the shortening of the ERP in all recording sites and the increase in ERP dispersion and ΣWOV were all attenuated, potently indicating the suppressed GP activity under the effect of A-803467. Since neurotransmission is not static and circumscribed, the $Na_V1.8$ blockade within the GPs on AF can have effects throughout the cardiac neuraxis. Due to the plasticity in the nervous system, based on present data, we cannot deduce that the observed effects may be limited only to the GPs. In fact, it may not be primarily mediated by GP blockade. Meanwhile, our previous study showed the colocalization of $Na_v1.5$ and $Na_v1.8$ when we transfected their cDNA separately into TSA201 cells. It would be more desirable if we could demonstrate this relationship in canine GP directly. However, our patch clamp study displayed that *SCN5A* could evidently increase *SCN10A* current in TSA201 cells, which can be blocked by A-803467. This phenomenon could indirectly explain the interaction between $Na_v1.5$ and $Na_v1.8$ to some extent.

Conclusions

In the present study, we found that the $Na_v1.8$ selective inhibitor could decrease the incidence of acute AF with suppressed electrical remodeling of atrial and PV myocardium in a RAP-induced AF model. $Na_v1.8$ could be a promising target in early AF, as GP activity were more important in early electrical

remodeling process of "AF begets AF" compared with progressed stages with prominent fibrosis and structural remodeling. In addition, we displayed that $Na_v1.8$ could probably interact with $Na_v1.5$, which may form a novel functional complex affecting cardiomyocyte and (or) cardiac GP properties, as shown in Figure 8. And it could be supported by our electrophysiological study with noticeable changes in I_{Na} and gating kinetics under A-803467. This novel sodium complex could be involved in AF and other *SCN10A*-related arrhythmias.

Acknowledgments

The authors are grateful to Judy Hefferon for creating the figures.

Sources of Funding

This study was supported by National Natural Science Foundation of China (No. 81670304), China; Independent Research Project of Wuhan University (No. 2042016kf0138), China; National Natural Science Foundation of China (No. 81530011), China; and the Masons of New York, Florida, Massachusetts, Connecticut, Maryland, Wisconsin, and Rhode Island, USA.

Disclosures

None.

References

1. Shivkumar K, Ajijola OA, Anand I, Armour JA, Chen PS, Esler M, De Ferrari G, Fishbein MC, Goldberger JJ, Harper RM, Joyner MJ, Khalsa SS, Kumar R, Lane R, Mahajan A, Po S, Schwartz PJ, Somers VK, Valderrabano M, Vaseghi M, Zipes DP. Clinical neurocardiology-defining the value of neuroscience-based cardiovascular therapeutics. *J Physiol*. 2016;594:3911–3954.
2. Choi EK, Shen MJ, Han S, Kim D, Hwang S, Sayfo S, Piccirillo G, Frick K, Fishbein MC, Hwang C, Lin SF, Chen PS. Intrinsic cardiac nerve activity and paroxysmal atrial tachyarrhythmia in ambulatory dogs. *Circulation*. 2010;121:2615–2623.
3. Patterson E, Po SS, Scherlag BJ, Lazzara R. Triggered firing in pulmonary veins initiated by in vitro autonomic nerve stimulation. *Heart Rhythm*. 2005;2:624–631.
4. Katritsis DG, Pokushalov E, Romanov A, Giazitzoglou E, Siontis GC, Po SS, Camm AJ, Ioannidis JP. Autonomic denervation added to pulmonary vein isolation for paroxysmal atrial fibrillation: a randomized clinical trial. *J Am Coll Cardiol*. 2013;62:2318–2325.
5. Pokushalov E, Romanov A, Katritsis DG, Artyomenko S, Shirokova N, Karaskov A, Mittal S, Steinberg JS. Ganglionated plexus ablation vs linear ablation in patients undergoing pulmonary vein isolation for persistent/long-standing persistent atrial fibrillation: a randomized comparison. *Heart Rhythm*. 2013;10:1280–1286.
6. Akopian AN, Sivilotti L, Wood JN. A tetrodotoxin-resistant voltage-gated sodium channel expressed by sensory neurons. *Nature*. 1996;379:257–262.
7. Akopian AN, Souslova V, England S, Okuse K, Ogata N, Ure J, Smith A, Kerr BJ, McMahon SB, Boyce S, Hill R, Stanfa LC, Dickenson AH, Wood JN. The tetrodotoxin-resistant sodium channel sns has a specialized function in pain pathways. *Nat Neurosci*. 1999;2:541–548.
8. London B. Whither art thou, SCN10A, and what art thou doing? *Circ Res*. 2012;111:268–270.
9. Hu D, Barajas-Martinez H, Pfeiffer R, Dezi F, Pfeiffer J, Buch T, Betzenhauser MJ, Belardinelli L, Kahlig KM, Rajamani S, DeAntonio HJ, Myerburg RJ, Ito H, Deshmukh P, Marieb M, Nam GB, Bhatia A, Hasdemir C, Haissaguerre M, Veltmann C, Schimpf R, Borggrefe M, Viskin S, Antzelevitch C. Mutations in SCN10A are responsible for a large fraction of cases of Brugada syndrome. *J Am Coll Cardiol*. 2014;64:66–79.
10. van den Boogaard M, Wong LY, Tessadori F, Bakker ML, Dreizehnter LK, Wakker V, Bezzina CR, t Hoen PA, Bakkers J, Barnett P, Christoffels VM. Genetic variation in T-box binding element functionally affects SCN5A/SCN10A enhancer. *J Clin Invest*. 2012;122:2519–2530.
11. van den Boogaard M, Smemo S, Burnicka-Turek O, Arnolds DE, van de Werken HJ, Klous P, McKean D, Muehlschlegel JD, Moosmann J, Toka O, Yang XH, Koopmann TT, Adriaens ME, Bezzina CR, de Laat W, Seidman C, Seidman JG, Christoffels VM, Nobrega MA, Barnett P, Moskowitz IP. A common genetic variant within *SCN10A* modulates cardiac *SCN5A* expression. *J Clin Invest*. 2014;124:1844–1852.
12. Delaney JT, Muhammad R, Shi Y, Schildcrout JS, Blair M, Short L, Roden DM, Darbar D. Common SCN10A variants modulate PR interval and heart rate response during atrial fibrillation. *Europace*. 2014;16:485–490.
13. Jabbari J, Olesen MS, Yuan L, Nielsen JB, Liang B, Macri V, Christophersen IE, Nielsen N, Sajadieh A, Ellinor PT, Grunnet M, Haunso S, Holst AG, Svendsen JH, Jespersen T. Common and rare variants in SCN10A modulate the risk of atrial fibrillation. *Circ Cardiovasc Genet*. 2015;8:64–73.
14. Savio-Galimberti E, Weeke P, Muhammad R, Blair M, Ansari S, Short L, Atack TC, Kor K, Vanoye CG, Olesen MS, LuCamp , Yang T, George AL Jr, Roden DM, Darbar D. SCN10A/Nav1.8 modulation of peak and late sodium currents in patients with early onset atrial fibrillation. *Cardiovasc Res*. 2014;104:355–363.
15. Qi B, Wei Y, Chen S, Zhou G, Li H, Xu J, Ding Y, Lu X, Zhao L, Zhang F, Chen G, Zhao J, Liu S. Nav1.8 channels in ganglionated plexi modulate atrial fibrillation inducibility. *Cardiovasc Res*. 2014;102:480–486.
16. Yu L, Scherlag BJ, Li S, Sheng X, Lu Z, Nakagawa H, Zhang Y, Jackman WM, Lazzara R, Jiang H, Po SS. Low-level vagosympathetic nerve stimulation inhibits atrial fibrillation inducibility: direct evidence by neural recordings from intrinsic cardiac ganglia. *J Cardiovasc Electrophysiol*. 2011;22:455–463.
17. Yu L, Scherlag BJ, Li S, Fan Y, Dyer J, Male S, Varma V, Sha Y, Stavrakis S, Po SS. Low-level transcutaneous electrical stimulation of the auricular branch of the vagus nerve: a noninvasive approach to treat the initial phase of atrial fibrillation. *Heart Rhythm*. 2013;10:428–435.
18. Li S, Scherlag BJ, Yu L, Sheng X, Zhang Y, Ali R, Dong Y, Ghias M, Po SS. Low-level vagosympathetic stimulation: a paradox and potential new modality for the treatment of focal atrial fibrillation. *Circ Arrhythm Electrophysiol*. 2009;2:645–651.
19. Vijayaragavan K, Powell AJ, Kinghorn IJ, Chahine M. Role of auxiliary beta1-, beta2-, and beta3-subunits and their interaction with Na(v)1.8 voltage-gated sodium channel. *Biochem Biophys Res Commun*. 2004;319:531–540.
20. Zhao J, O'Leary ME, Chahine M. Regulation of Nav1.6 and Nav1.8 peripheral nerve Na+ channels by auxiliary beta-subunits. *J Neurophysiol*. 2011;106:608–619.
21. Yang T, Atack TC, Stroud DM, Zhang W, Hall L, Roden DM. Blocking Scn10a channels in heart reduces late sodium current and is antiarrhythmic. *Circ Res*. 2012;111:322–332.
22. Nishida K, Maguy A, Sakabe M, Comtois P, Inoue H, Nattel S. The role of pulmonary veins vs. autonomic ganglia in different experimental substrates of canine atrial fibrillation. *Cardiovasc Res*. 2011;89:825–833.
23. Nattel S, Dobrev D. Electrophysiological and molecular mechanisms of paroxysmal atrial fibrillation. *Nat Rev Cardiol*. 2016;10:575–590.
24. Patterson E, Lazzara R, Szabo B, Liu H, Tang D, Li YH, Scherlag BJ, Po SS. Sodium-calcium exchange initiated by the Ca^{2+} transient: an arrhythmia trigger within pulmonary veins. *J Am Coll Cardiol*. 2006;47:1196–1206.
25. Tan AY, Zhou S, Ogawa M, Song J, Chu M, Li H, Fishbein MC, Lin SF, Chen LS, Chen PS. Neural mechanisms of paroxysmal atrial fibrillation and paroxysmal atrial tachycardia in ambulatory canines. *Circulation*. 2008;118:916–925.
26. Lu Z, Scherlag BJ, Lin J, Niu G, Fung KM, Zhao L, Ghias M, Jackman WM, Lazzara R, Jiang H, Po SS. Atrial fibrillation begets atrial fibrillation: autonomic mechanism for atrial electrical remodeling induced by short-term rapid atrial pacing. *Circ Arrhythm Electrophysiol*. 2008;1:184–192.
27. Po SS, Scherlag BJ, Yamanashi WS, Edwards J, Zhou J, Wu R, Geng N, Lazzara R, Jackman WM. Experimental model for paroxysmal atrial fibrillation arising at the pulmonary vein-atrial junctions. *Heart Rhythm*. 2006;3:201–208.
28. Hou Y, Scherlag BJ, Lin J, Zhang Y, Lu Z, Truong K, Patterson E, Lazzara R, Jackman WM, Po SS. Ganglionated plexi modulate extrinsic cardiac autonomic nerve input: effects on sinus rate, atrioventricular conduction, refractoriness, and inducibility of atrial fibrillation. *J Am Coll Cardiol*. 2007;50:61–68.
29. Boucher M, Dubray C, Li JH, Paire M, Duchene-Marullaz P. Influence of pentobarbital and chloralose anesthesia on quinidine-induced effects on atrial

refractoriness and heart rate in the dog. *J Cardiovasc Pharmacol*. 1991;17:199–206.

30. Chiba S, Tsuboi M. Dominant anti-vagal effect of pentobarbital on cardiac responses to intracardiac autonomic nerve stimulation in the dog. *Jpn J Pharmacol*. 2001;86:248–250.
31. Yu L, Scherlag BJ, Sha Y, Li S, Sharma T, Nakagawa H, Jackman WM, Lazzara R, Jiang H, Po SS. Interactions between atrial electrical remodeling and autonomic remodeling: how to break the vicious cycle. *Heart Rhythm*. 2012;9:804–809.
32. Lu Z, Scherlag BJ, Lin J, Yu L, Guo JH, Niu G, Jackman WM, Lazzara R, Jiang H, Po SS. Autonomic mechanism for initiation of rapid firing from atria and pulmonary veins: evidence by ablation of ganglionated plexi. *Cardiovasc Res*. 2009;84:245–252.
33. Scherlag BJ, Yamanashi W, Patel U, Lazzara R, Jackman WM. Autonomically induced conversion of pulmonary vein focal firing into atrial fibrillation. *J Am Coll Cardiol*. 2005;45:1878–1886.
34. Chevrier P, Vijayaragavan K, Chahine M. Differential modulation of Nav1.7 and Nav1.8 peripheral nerve sodium channels by the local anesthetic lidocaine. *Br J Pharmacol*. 2004;142:576–584.
35. Jarvis MF, Honore P, Shieh CC, Chapman M, Joshi S, Zhang XF, Kort M, Carroll W, Marron B, Atkinson R, Thomas J, Liu D, Krambis M, Liu Y, McGaraughty S, Chu K, Roeloffs R, Zhong C, Mikusa JP, Hernandez G, Gauvin D, Wade C, Zhu C, Pai M, Scanio M, Shi L, Drizin I, Gregg R, Matulenko M, Hakeem A, Gross M, Johnson M, Marsh K, Wagoner PK, Sullivan JP, Faltynek CR, Krafte DS. A-803467, a potent and selective Nav1.8 sodium channel blocker, attenuates neuropathic and inflammatory pain in the rat. *Proc Natl Acad Sci USA*. 2007;104:8520–8525.
36. Verkerk AO, Remme CA, Schumacher CA, Scicluna BP, Wolswinkel R, de Jonge B, Bezzina CR, Veldkamp MW. Functional Nav1.8 channels in intracardiac neurons: the link between SCN10A and cardiac electrophysiology. *Circ Res*. 2012;111:333–343.
37. Behr ER, Savio-Galimberti E, Barc J, Holst AG, Petropoulou E, Prins BP, Jabbari J, Torchio M, Berthet M, Mizusawa Y, Yang T, Nannenberg EA, Dagradi F, Weeke P, Bastiaenan R, Ackerman MJ, Haunso S, Leenhardt A, Kaab S, Probst V, Redon R, Sharma S, Wilde A, Tfelt-Hansen J, Schwartz P, Roden DM, Bezzina CR, Olesen M, Darbar D, Guicheney P, Crotti L; Consortium UK, Jamshidi Y. Role of common and rare variants in SCN10A: results from the Brugada syndrome QRS locus gene discovery collaborative study. *Cardiovasc Res*. 2015;106:520–529.
38. Fukuyama M, Ohno S, Makiyama T, Horie M. Novel SCN10A variants associated with Brugada syndrome. *Europace*. 2015;18:905–911.
39. Facer P, Punjabi PP, Abrari A, Kaba RA, Severs NJ, Chambers J, Kooner JS, Anand P. Localisation of SCN10A gene product Na(v)1.8 and novel pain-related ion channels in human heart. *Int Heart J*. 2011;52:146–152.
40. Iio C, Ogimoto A, Nagai T, Suzuki J, Inoue K, Nishimura K, Uetani T, Okayama H, Okura T, Shigematsu Y, Tabara Y, Kohara K, Miki T, Hamada M, Higaki J. Association between genetic variation in the SCN10A gene and cardiac conduction abnormalities in patients with hypertrophic cardiomyopathy. *Int Heart J*. 2015;56:421–427.